Commun. Comput. Chem doi: 10.4208/cicc.2014.v2.n3.1

#### COMMUNICATION

## First-Principles Study on the Cubic CaSiO<sub>3</sub> (001) Surface

Kun Yang<sup>1\*</sup>, Li Yao<sup>1</sup>, Xiao-Zhen Wang<sup>1</sup>, Zhuo Feng<sup>2</sup> and Li Li<sup>3</sup>

Received 1 Sep 2014; Accepted (in revised version) 24 Sep 2014

**Abstract**: The geometric and electronic structure of the cubic CaSiO<sub>3</sub> (001) surfaces have been studied using first-principles density functional theory (DFT) calculations. Two different terminations, CaO- and SiO<sub>2</sub>- terminated surfaces, were investigated. It has been found that Ca atom has the largest relaxation for both kinds of terminations, and the rumpling of the CaO-terminated surface is much larger than that of the SiO<sub>2</sub>-terminated surface. The band gaps of the CaO- and SiO<sub>2</sub>-terminated surfaces were calculated to be smaller than that of the CaSiO<sub>3</sub> bulk. It was also shown that the SiO<sub>2</sub>-terminated surface has a lower energy than the CaO-terminated surface.

AMS subject classifications: 68U05, 68U07

Keywords: CaSiO<sub>3</sub>, surface structure, density functional theory, electronic structure

#### 1. Introduction

Composition estimates of the Earth reveal that the MgO-FeO-CaO-SiO<sub>2</sub>-Al<sub>2</sub>O<sub>3</sub> system could occupy ~ 99% of the mantle volume [1]. In the Earth's lower mantle, the Ca-bearing phase is present in the CaSiO<sub>3</sub> perovskite form [2,3], which is the third most important phase. Under ambient conditions, however, CaSiO<sub>3</sub> perovskite is not stable and it could readily convert to glass on the release of pressure. At 490-580 K and 27-72 GPa, CaSiO<sub>3</sub> perovskite undergoes

<sup>&</sup>lt;sup>1</sup>Department of Physics, Dalian Maritime University, Dalian, 116026, China.

<sup>&</sup>lt;sup>2</sup>Navigation College, Dalian Maritime University, Dalian, 116026, China.

<sup>&</sup>lt;sup>3</sup>Marine Engineering College, Dalian Maritime University, Dalian, 116026, China.

<sup>\*</sup> Corresponding author, *E-mail address*: yangk@dlmu.edu.cn(K. Yang), Tel: +86-411-84729331 Fax: +86-411-84724335

phase transformation from tetragonal symmetry to ideal cubic structure [4].

Density functional theory (DFT) studies have been carried out on the lattice structure, sound velocity and elastic properties of bulk CaSiO<sub>3</sub> in tetragonal and orthorhombic phases as well as in low-symmetry cubic phase [5-7]. However, the structural and electronic properties of the CaSiO<sub>3</sub> surface are rarely investigated, despite the fact that the surfaces of other Ca-bearing perovskites, e.g. CaTiO<sub>3</sub> [8-10] and CaZrO<sub>3</sub> [11], have been well studied. In this work, first-principles calculations were carried out on the systematic study of the geometric and electronic properties of cubic CaSiO<sub>3</sub> (001) surface with CaO and SiO<sub>2</sub> terminations. The rumpling of the surfaces, band structures and energetic properties of the two kinds of terminations are compared to each other.

## 2. Computational details

The DFT calculations presented in this work were carried out within the generalized gradient approximation (GGA), using the projector-augmented wave (PAW) method and a plane-wave basis set, as implemented in the Vienna *ab initio* Simulation Package (VASP) [12,13]. The plane-wave energy cutoff is 600 eV for all calculations and the Brillouin zone integration is performed using the Monkhorst-Pack scheme with Ca (3s, 3p, 4s), Si (3s, 3p), and O(2s, 2p) treated as valence.

#### 3. Results and discussion

# 3.1 Structural properties

We first optimized lattice constant of cubic bulk CaSiO<sub>3</sub> with the 12×12×12 k-point mesh. The computed lattice constant of cubic CaSiO<sub>3</sub> is 3.604 Å, which is in good agreement with the equation of state (EOS) determined lattice constant of cubic CaSiO<sub>3</sub> in previous experimental study (3.572 Å) [14] and other GGA calculated result (3.546 Å) [5]. This theoretical lattice constant was used in all surface calculations presented here. Two symmetrical repeat-slab surface models with space group P4/mmm were used for the calculations: CaO-terminated and SiO<sub>2</sub>-terminated surfaces. For the CaO-terminated surface, the unit slab consists of four CaO and three SiO<sub>2</sub> layers, so that the slab is terminated with CaO layer on either surface. Similarly, for the SiO<sub>2</sub>-terminated slab, there are three CaO and four SiO<sub>2</sub> layers in the unit slab, so SiO<sub>2</sub> layers are terminated on both outmost surfaces. For each unit slab, there are seven alternating CaO and SiO<sub>2</sub> layers, together with a 12 Å vacuum separation to minimize possible interactions between neighboring slab surfaces. For both slabs, the in-plane lattice constant is set to the computed cubic equilibrium value 3.604 Å, and the atomic

displacements perpendicular to the surface are fully relaxed using a 12×12×2 k-point mesh.

Because of the P4/mmm symmetry, there is a mirror reflection on the central layer of each slab, thus the relaxations of the atoms on top and bottom layers are of the same amplitude but along opposite directions, and so are other symmetrical layers. **Table 1** lists the atomic displacements  $\delta z$  of the outmost three layers. For CaO-terminated surface, the surface layer Ca atom and O atom move toward opposite directions, i.e. the Ca atom moves inward to the central layer and the O atom relaxes outward to the vacuum region. The surface Ca atom has a large relaxation of 3.44% of the bulk lattice constant, which is the greatest relaxation of all atoms of both layers. For the SiO2-terminated surface, the surface Si atom relaxes remarkably toward the central layer by 2.64%. However, the largest relaxation is not on the surface layer atoms but on the second layer Ca atom, which relaxes outward (toward the surface) by 2.73%. It is noted that the Ca and Si atoms relax toward opposite directions with respect to the same-layer O atoms except the second layer of CaO-terminated slab. The Ca and Si atoms relax much more remarkably than O atoms in all layers. It is also found that the displacements of Ca atoms are much larger than those of Si atoms in both surface slabs, suggesting that Ca atom is much easier to relax than Si atom.

**Table 1.** Calculated atomic displacements (relative to ideal positions)  $\delta z$  of the top three layers of CaO- and SiO<sub>2</sub>-terminated CaSiO<sub>3</sub> surfaces. Units are in percent of theoretical CaSiO<sub>3</sub> cubic bulk lattice constant (a=3.604 Å). Positive values refer to displacements towards the surface.

layer	CaO-terminated		SiO <sub>2</sub> -1	SiO <sub>2</sub> -terminated	
	Atom	$\delta z$	Atom	$\delta z$	
1	Ca	-3.44	Si	-2.64	
	Ο	0.79	O	1.35	
2	Si	1.16	Ca	2.73	
	O	0.03	O	-0.09	
3	Ca	-0.45	Si	-0.35	
	Ο	0.14	O	0.20	

In **Table 2**, we show the surface relaxation parameters. Surface rumpling parameter s measures the outward displacement of the surface layer O atom with respect to the surface layer Ca or Si atom.  $\Delta d_{12}$  is the change of the first interlayer spacing, as measured from the surface to the second layer Ca and Si atoms z-coordinate, and  $\Delta d_{23}$  is similar with  $\Delta d_{12}$  but between the second and the third layers. It can be seen from **Table 2** that the rumplings of CaO-terminated and SiO<sub>2</sub>-terminated surfaces are very close, i.e. the rumpling of CaO-terminated surface is only slightly larger than that of SiO<sub>2</sub>-terminated surface. Thus, our calculation suggests that the CaSiO<sub>3</sub> (001) surface could be almost even rough when it is terminated with either CaO or SiO<sub>2</sub> termination. Parameter  $\Delta d_{12}$  is negative for both kinds of

terminations, indicating that the distance between the first and the second layers becomes smaller by comparison with its bulk value. The absolute value of  $\Delta d_{12}$  for SiO<sub>2</sub>-terminated surface is larger than that of CaO-terminated surface, suggesting that the distance between the surface layer and the second layer is much more reduced for SiO<sub>2</sub>-terminated surface. On the contrary,  $\Delta d_{23}$ , the distance between the second and the third layers expands for both terminations, and the expansion is larger for SiO<sub>2</sub>-terminated surface than for CaO-terminated surface.

**Table 2.** Surface relaxation parameters for CaO- and SiO<sub>2</sub>-terminated CaSiO<sub>3</sub> surface. Values are in percent of theoretical CaSiO<sub>3</sub> cubic bulk lattice constant (*a*=3.604 Å)

Surface	s	$\Delta d_{12}$	$\Delta d$ 23	
CaO-terminated	4.23	-4.60	1.61	
SiO <sub>2</sub> -terminated	3.99	-5.37	3.08	

### 3.2 Band structures and partial density of states

In **Figure 1**, we show the calculated band structures of CaO- and SiO<sub>2</sub>-terminated relaxed surfaces together with the band structure of bulk cubic CaSiO<sub>3</sub>. The cubic bulk CaSiO<sub>3</sub> is calculated to have an indirect band gap of 3.55 eV, with the valance band maximum locating at R point and the conduction band minimum at Γ point as presented in **Figure 1(a)**. As can be seen from **Figure 1(b)**, the top valence band of CaO-terminated surface is flat between X and M points, with the calculated band gap of 2.57 eV. This gap value shows ~1 eV reduction with respect to its bulk band gap value. For the band structure of the SiO<sub>2</sub>-terminated surface in **Figure 1(c)**, the calculated band gap is 1.62 eV, which is more reduced compared to its bulk value. The driving force for this relatively larger gap reduction is partially due to the tendency of the upper valence band states intruding upward near the M point. In addition, the lower conduction bands of SiO<sub>2</sub>-terminated surface locate even lower than those of the CaO-terminated one, which narrows the band gap much more.

To clarify the reason of the reduced gaps of the surface slabs compared with the bulk, we then calculated the partial density of states (PDOS) of CaO- and SiO<sub>2</sub>-terminated CaSiO<sub>3</sub> surfaces, as is shown in **Figure 2**. For both two surface types, O 2p states occupy the topmost valence bands, and Si 3s and 3p states contribute most to the lowest conduction bands. It is obvious that the central layer Si 3s and 3p PDOS of the CaO-termination is quite similar to the third layer Si 3s and 3p PDOS of the SiO<sub>2</sub>-termination. However, the second layer Si 3s and 3p PDOS of the SiO<sub>2</sub>-termination is very different to the surface layer Si 3s and 3p PDOS of the SiO<sub>2</sub>-termination. The SiO<sub>2</sub>-termination surface layer Si 3s and 3p has relatively large PDOS in the lowest conduction band area, ranging from 1.62 eV to ~4 eV, which suggests

that the surface Si 3s and 3p PDOS intrusion into the lower part is the main reason of the large band gap reduction of the SiO<sub>2</sub>-terminated surface with respect to that of the CaSiO<sub>3</sub> bulk.

## 3.3 Surface energies

In order to compare the energetic stability of CaO-terminated and SiO<sub>2</sub>-terminated surfaces, we calculated their surface energies using the standard approach of the surface energy calculation [8,11,15]. The surface energy  $E_s$  is defined as the sum of the cleavage energy  $(E_{cle})$  and relaxation energy  $(E_{rel})$ :

$$E_s(I) = E_{cle} + E_{rel}(I) \tag{1}$$

where "I" denotes CaO or SiO<sub>2</sub> terminations. Since the two terminations form simultaneously under cleavage, it is assumed that the relevant cleavage energy is the same for both terminations:

$$E_{cle} = \frac{1}{4} \left[ E_{slab}^{unrel}(C_a O) + E_{slab}^{unrel}(SiO_2) - 7E_{bulk} \right] \tag{2}$$

Where  $E_{slab}^{unrel}(C_aO)$  and  $E_{slab}^{unrel}(SiO_2)$  are the energies for unrelaxed CaO- and SiO<sub>2</sub>-terminated slabs respectively, and  $E_{bulk}$  is the cubic CaSiO<sub>3</sub> bulk unit cell energy. The factor 1/4 is due to the fact that four surfaces are created during the cleavage, and the factor 7 is introduced because the two seven-layer slabs represent seven bulk unit cells. The relaxation energy is defined as the energy change after relaxation:

$$E_{rel}(I) = \frac{1}{2} \left[ E_{slab}^{rel}(I) - E_{slab}^{unrel}(I) \right]$$
 (3)

Where  $E_{slab}^{rel}(I)$  is the slab energy after relaxation. Since both top and bottom surfaces of the

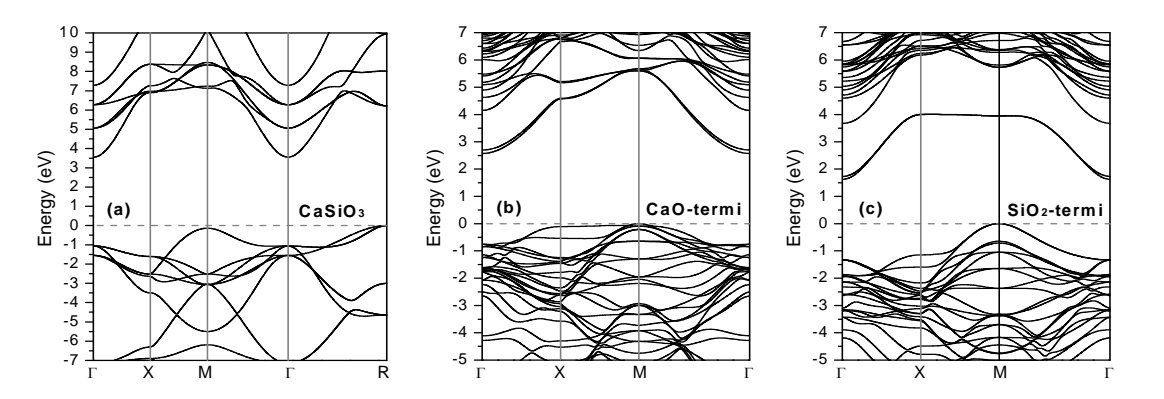


Figure 1: Band structures of CaSiO<sub>3</sub> cubic bulk (a), CaO-terminated surface (b) and SiO<sub>2</sub>-terminated surface (c)

slab are relaxed, a factor 1/2 is introduced in Equation 3. The surface energies we obtained are  $E_s(C_aO)=0.98eV$  and  $E_s(SiO_2)=0.87eV$ , respectively, which indicates that the SiO<sub>2</sub>-terminated surface is energetically favorable. In other words, there could be more SiO<sub>2</sub> terminations on CaSiO<sub>3</sub> (001) surface rather than CaO terminated ones.

#### 4. Conclusion

We have found from first-principles DFT calculations that for the cubic CaSiO<sub>3</sub> (001) surface, the rumpling of CaO-terminated surface is larger than that of the SiO<sub>2</sub>-terminated one. Ca atoms relax much more than Si and O atoms for both kinds of surface termination. Compared with the band gap of cubic bulk CaSiO<sub>3</sub>, the band gap of SiO<sub>2</sub>-terminated surface reduces much more than CaO termination, which is mainly due to the downward of the conduction band state of surface layer Si 3s and 3p states. Energy calculation reveals that the two models of surface terminations has relative close surface stabilities, with the SiO<sub>2</sub>-terminated surface more stable than the CaO-terminated one.

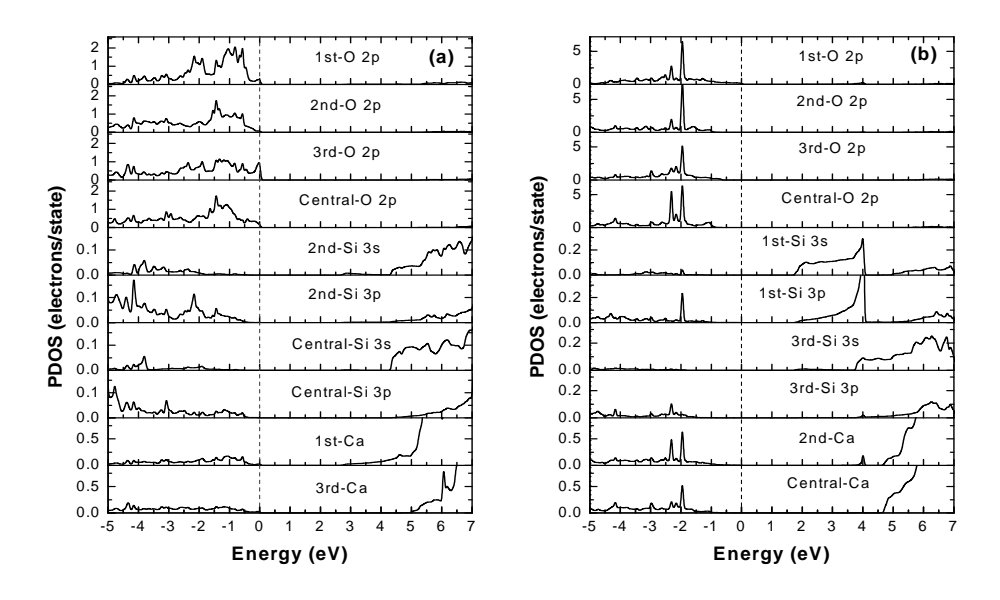


Figure 2: PDOS of atoms in each layer: (a) CaO-terminated surface and (b) SiO<sub>2</sub>-terminated surface.

# Acknowledgment

The authors thank the National Natural Science Foundation of China (11047110 and 11304028), the Fundamental Research Funds for the Central Universities (2011JC021,

3132014228 and 3132014337) and College Students Innovation Project of DMU for financial support.

#### References

- [1] D. L. Anderson, Composition of the Earth, Science, 243 (1989), 367-370.
- [2] K. Hirose, Y. Fei, Y. Ma and H. K. Mao, The fate of subducted basaltic crust in the Earth's lower mantle, Nature, 397 (1999), 53-56.
- [3] S. Ono, Experimental constraints on the temperature profile in the lower mantle, Phys. Earth Planet. In., 170 (2008), 267-273.
- [4] T. Komabayashi, K. Hirose, N. Sata, Y. Ohishi and L. S. Dubrovinsky, Phase transition in CaSiO<sub>3</sub> perovskite, Earth Planet. Sc. Lett., 260 (2007), 564-569.
- [5] R. Caracas and R. M. Wentzcovitch, Theoretical determination of the structures of CaSiO<sub>3</sub> perovskites, Acta Crystallogr., Sect. B, 62 (2006), 1025-1030.
- [6] Z. J. Liu, S. Q. Duan, J. Yan, X. W. Sun, C. R. Zhang and Y. D. Chu, Theoretical investigations of the physical properties of tetragonal CaSiO<sub>3</sub> perovskite, Solid State Commun., 150 (2010), 943-948.
- [7] S. Ono, Elastic Properties of CaSiO<sub>3</sub> Perovskite from ab initio Molecular Dynamics, Entropy, 15 (2013), 4300-4309.
- [8] K. Yang, C. L. Wang, J. C. Li, C. Zhang, Q. Z. Wu, Y. F. Zhang, N. Yin and X. Y. Liu, Surface rumpling of cubic CaTiO<sub>3</sub> from density functional theory, Chin. Phys., 15 (2006), 1580-1584.
- [9] R. I. Eglitis and D. Vanderbilt, Ab initio calculations of the atomic and electronic structure of CaTiO<sub>3</sub> (001) and (011) surfaces, Phys. Rev. B, 78 (2008), 155420.
- [10] Y. X. Wang, M. Arai, T. Sasaki and C. L. Wang, First-principles study of the (001) surface of cubic CaTiO<sub>3</sub>, Phys. Rev. B, 73 (2006), 035411.
- [11] M. G. Brik, C. G. Ma and V. Krasnenko, First-principles calculations of the structural and electronic properties of the cubic CaZrO<sub>3</sub> (001) surfaces, Surf. Sci., 608 (2013), 146-153.
- [12] G. Kresse and J. Furthmüller, Efficient iterative schemes for ab initio total-energy calculations using a plane-wave basis set, Phys. Rev. B, 54 (1996), 11169-11186.
- [13] G. Kresse and D. Joubert, From ultrasoft pseudopotentials to the projector augmented-wave method, Phys. Rev. B, 59 (1999), 1758-1775.
- [14] S. H. Shim, T. S. Duffy and G. Shen, The stability and P–V–T equation of state of CaSiO<sub>3</sub> perovskite in the Earth's lower mantle, J. Geophys. Res., 105 (2000), 25955-25968.
- [15] E. Heifets, R. I. Eglitis, E. A. Kotomin, J. Maier and G. Borstel, *Ab initio* modeling of surface structure for SrTiO<sub>3</sub> perovskite crystals, Phys. Rev. B, 64 (2001), 235417.